# High Efficiency DC-DC Converters for Battery-Operated Systems with Energy Management

**Robert Erickson and Dragan Maksimovic**
**Department of Electrical and Computer Engineering**
**University of Colorado, Boulder 80309-0425**

**Abstract—** Dc-dc converters suitable for use in battery-powered electronic equipment with energy management are discussed. To realize the benefits of energy management, these converters must be capable of maintaining regulation of their output voltages at no load, while maintaining high efficiency.

Variable frequency operation is shown to give an improvement in efficient operating range of approximately two orders of magnitude. Proportionality of the battery and load currents can be maintained over approximately five orders of magnitude, with minimum battery currents of less than 100μA and maximum load currents approaching 10A.

Steady-state and small-signal ac characteristics of converters operating with variable-frequency control are tabulated, and an ac two-port model is described.

## 1. Introduction

Energy management in battery-operated systems can allow greater capabilities in energy-limited systems. Elements with high instantaneous power consumption can be used, such as transmitters, microprocessors, backlit displays, and flash memory, provided that they are switched to a low-power standby mode when not needed. The use of low-voltage power supplies (3.3V or less) to reduce power consumption can also allow greater capability, at the expense of lower noise margins and a requirement for better voltage regulation. In the standby mode, some payloads are switched off, while others operate with reduced capability and at very low power consumption, listening for a wake-up signal.

Battery leakage currents are typically a fraction of a microampere; this could be taken as an ultimate goal for the standby mode current. Standby currents of one to two orders of magnitude greater than this figure, in the 10-100μA range, would yield good performance for many applications. Meeting these goals requires improvements in both payload and dc-dc converter technologies.

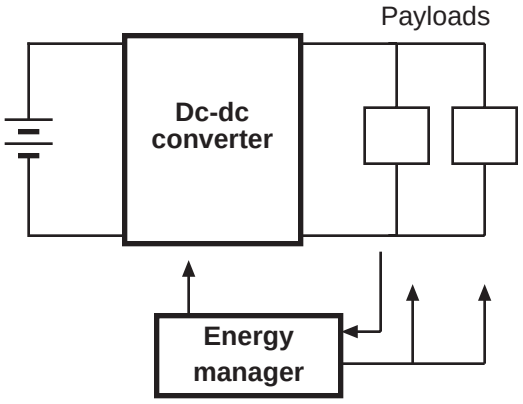


*Fig. 1. A simple energy management system for a battery-powered mobile system.*

To fully realize a battery-powered energy management system, dc-dc converters are needed which meet new requirements. Simply turning off the converter in the standby mode is insufficient, since part of the payload must continue to operate. Hence, the converter must maintain regulation of the load voltage with zero load current. High converter efficiency is required over many orders of magnitude variation in the load power, typically from tens of microwatts to tens of watts. Since system volume and weight are dominated by the batteries rather than the converter, high efficiency is more important than converter size and weight; nonetheless, minimization of converter volume and weight is also a goal.

Conventional fixed-frequency dc-dc converters cannot meet these requirements. A conventional 0-25W, 4.8V input, 3.3V output fixed frequency design is examined in section 2, and is shown to exhibit high efficiency for $25\text{W} \geq P_{out} \geq 0.2\text{W}$. The current drawn from the battery at no load (standby current) is 5mA. In addition to exhibiting high fixed (load-independent) losses, this approach is unable to regulate its output at zero load.

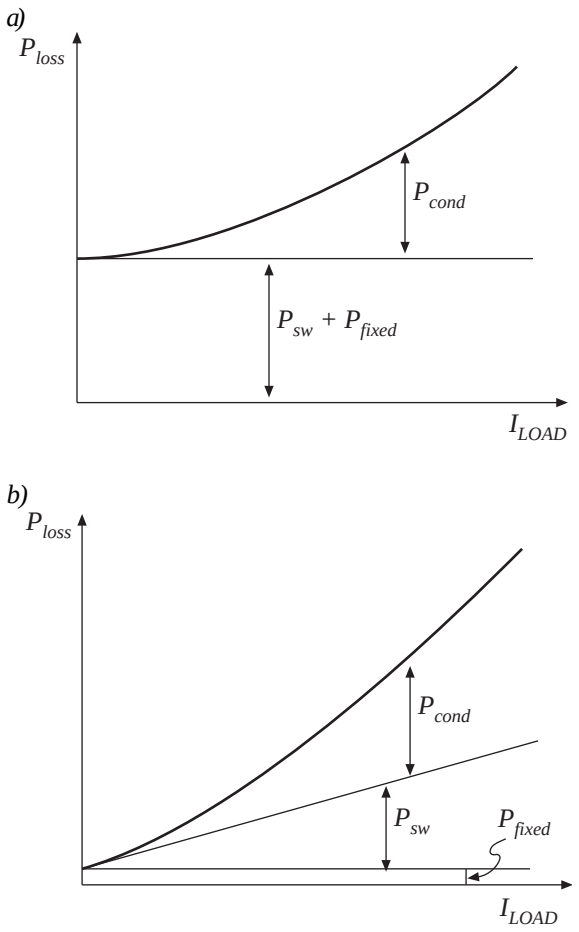


*Fig. 2. Variation of converter power losses with load current: (a) in a conventional fixed-frequency converter; (b) with switching frequency proportional to load current.*

As illustrated in Fig. 2(a), a conventional dc-dc converter contains substantial fixed losses, which are independent of the load current. These fixed losses lead to a significant battery current at no load. As discussed in section 2, the total converter power losses $P_{loss}$ can be expressed as

$$P_{loss} = P_{cond}(I_{load}) + W_{sw} f_{sw} + P_{fixed} \qquad (1)$$

where $P_{cond}$ is the converter conduction loss, directly dependent on load current, $W_{sw}$ is the energy lost during the transistor switch-on and switch-off transitions, dependent on the switching frequency $f_{sw}$, and $P_{fixed}$ is the fixed loss, dependent on neither load current nor switching frequency. The switching loss $W_{sw}f_{sw}$ accounts for nearly all of the fixed loss. This suggests that one should reduce the switching frequency $f_{sw}$ as the load current decreases, causing the frequency-dependent losses to vary with load as in Fig. 2(b). Decrease of the converter standby current by one to two orders of magnitude is feasible using such a scheme. The performance, design, and optimization of variable-frequency converters for this application are summarized in section 3. With this approach, converter fixed losses can be reduced by nearly two orders of magnitude, with a no-load battery current of less than 100μA [3,4]. With the variable-frequency approach, standby performance is limited by semiconductor device leakage currents, power controller chip standby current, and payload standby current.

The characteristics of converters operating in discontinuous conduction mode with variable frequency control are tabulated in section 4. A small-signal equivalent circuit model is also given, which is solved to yield the small-signal control transfer functions of these converters. The results are summarized in section 5, and some directions for future R&D are suggested.

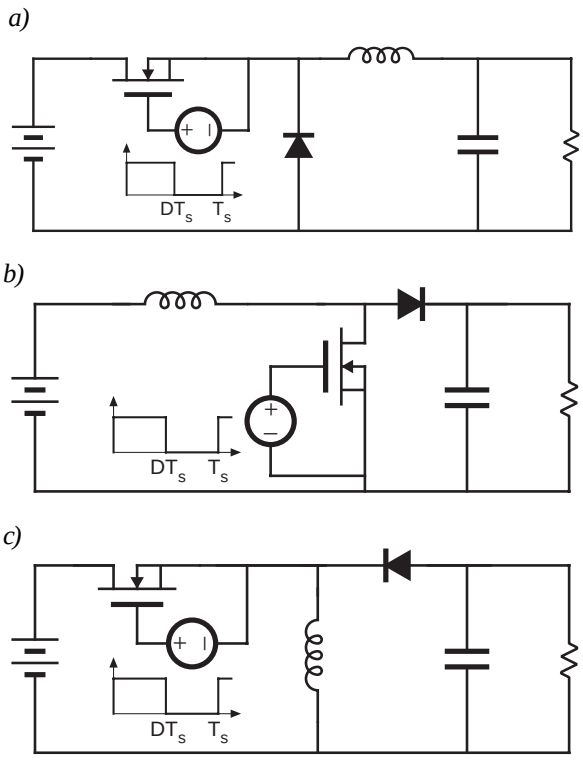


*Fig. 3. Basic dc-dc switching converter circuits: (a) buck, (b) boost, (c) buck-boost.*

## 2. Performance of the conventional fixed-frequency approach

Several basic dc-dc converter circuits are shown in Fig. 3. The buck converter, Fig. 3(a), reduces the dc voltage magnitude, and is used as an example here to reduce a four-cell battery voltage (4.8V minimum) to a regulated 3.3V dc. The boost converter, Fig. 3(b), is commonly used to increase the voltage magnitude, and can interface a one- or two-cell battery pack to a 5Vdc load. The buck-boost converter, Fig. 3(c), inverts the voltage polarity. All three converters exhibit similar loss behavior.

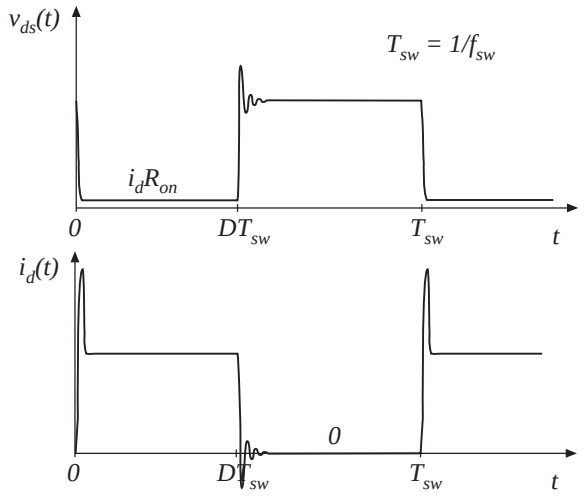


*Fig. 4. Typical MOSFET voltage and current waveforms in a conventional dc-dc converter operating in continuous conduction mode.*

Typical MOSFET voltage and current waveforms are given in Fig. 4. These waveforms lead to several types of power loss, listed in Table 1. Conduction losses are directly dependent on the load current, and nearly independent of switching frequency. An example is the power loss due to current flowing through the MOSFET on-resistance and the diode forward voltage drop. Conduction losses dominate the other types of loss at maximum load power, but have little effect at light load or under standby conditions.

Switching losses are nearly independent of the value of the load current, but depend directly on the converter switching frequency. An example is the loss due to the energy stored in the MOSFET output (drain-to-source) capacitance. When the MOSFET is switched on, this capacitance is shorted out, and the energy stored in it is lost. The total switching power loss is equal to the total energy lost during the turn-on and turn-off switching transitions, multiplied by the switching frequency $f_{sw}$. The various sources of switching loss in a conventional dc-dc switching converter are now quite well documented in the literature; see, for ex., [2,5]. Depending on the value of the switching frequency, switching losses may or may not be significant at full load. However, at light load and under standby conditions, the switching losses are a serious source of power loss in a fixed-frequency converter.

**Table 1. Origins of Loss in a Conventional Fixed-Frequency Converter**

| |
|---|
| ***Load-Dependent (Conduction) Losses*** |
| MOSFET on resistance |
| Diode forward voltage drop |
| Inductor winding resistance |
| Capacitor equivalent series resistance |
| ***Frequency-Dependent (Switching) Losses*** |
| MOSFET output capacitance |
| MOSFET gate capacitance |
| Diode capacitance |
| Diode stored minority charge |
| Inductor and transformer core loss |
| Snubber loss |
| Gate driver losses |
| ***Other Fixed Losses*** |
| Controller standby current |
| MOSFET, diode, and capacitor leakage currents |

Other sources of fixed loss, independent of both switching frequency and load current, include the power supply controller standby current and the leakage currents of the transistors, diode, and filter capacitors. These losses remain, even when the switching converter is shut off. They represent the minimum power which can be drawn from the battery, and should be minimized.

At the low voltage levels typical of battery-operated equipment, synchronous rectification is often used. As shown in Fig. 5, the diode is replaced by a MOSFET. A control circuit gates the MOSFET on and off at the times when the diode would have switched. If the MOSFET is sufficiently large, then the MOSFET forward voltage drop is less than the diode forward voltage drop would have been, and the conduction losses are reduced. Synchronous rectification is of significant benefit when the battery or load voltage is comparable to the diode forward voltage drop, as is the case in most battery-operated equipment. An added benefit is the reduction of leakage currents, since the MOSFET leakage current (on the order of one microampere at room temperature) is much lower than the leakage current

in a low-$V_F$ schottky diode (in the milliampere range). The gate drive control circuit should be carefully designed, to ensure that the transistor is correctly switched on and off in the discontinuous conduction mode.

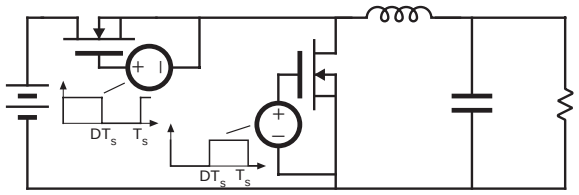


*Fig. 5. Buck converter with synchronous rectification.*

Efficiency and battery current are plotted vs. load power in Figures 6 and 7, for a well-designed conventional fixed-frequency switching converter in a typical application. A buck converter, Fig. 3(a), is used to supply a regulated 3.3V to a 0-25W load, from a four-cell battery pack having a minimum voltage of 4.8V. The switching frequency is a fixed 100kHz. A logic-level MOSFET (MTP15N05EL) and schottky diode (80SQ) are assumed. The ferrite inductor has the value 10µH with a winding resistance of 10mΩ. The controller current is assumed to be a fixed 75µA, plus 20nC*$f_{sw}$. All losses listed in Table 1 are modeled, and it is assumed that the converter regulates the output voltage to 3.3V over the entire output power range of 0-25W.

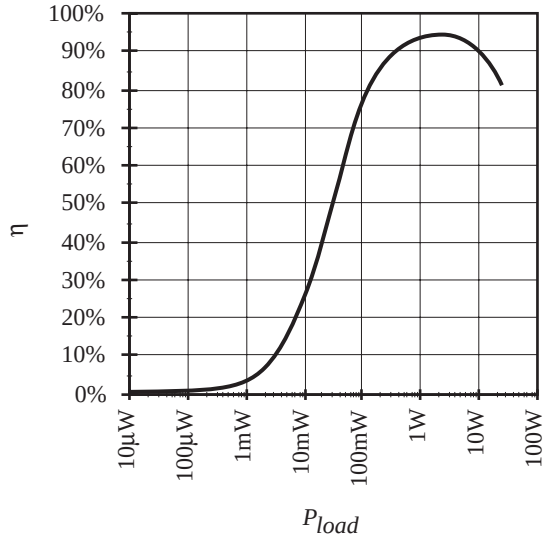


*Fig. 6. Predicted converter efficiency vs. output power, conventional fixed frequency converter.*

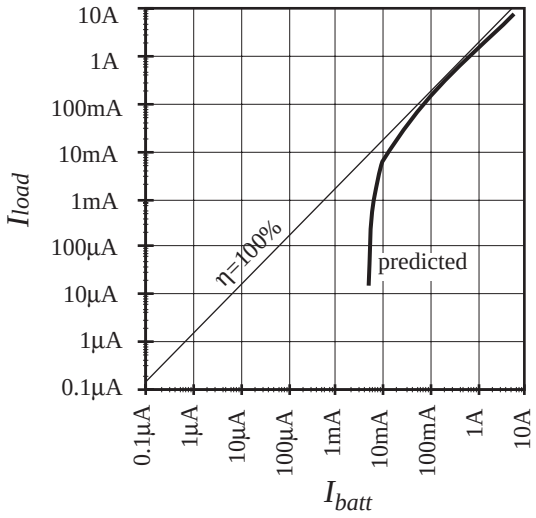


*Fig. 7. Predicted converter input current vs. output current, conventional fixed frequency converter.*

It can be seen from Fig. 6 that the predicted converter efficiency is above 80% for load powers in the range 0.2W – 25W. However, the efficiency is poor at lower power levels. More illuminating is Fig. 7, in which the battery current is plotted vs. load current. The minimum battery current is approximately 5mA, regardless of the load current. Even with the load disconnected, the converter requires 5mA of battery current to maintain regulation of the converter output voltage. A well-designed dc-dc converter using the conventional fixed-frequency approach is able to maintain high efficiency over less than three orders of magnitude of load powers. Apparently, reducing the load current to the microampere range does not yield corresponding reductions in battery current, and hence the goals of energy management are not realized.

## 3. Performance of the variable-frequency approach

According to Eq. (1), the switching loss $W_{sw}\ f_{sw}$ is a fixed loss when the switching frequency $f_{sw}$ is constant as in the conventional approach. However, if the switching frequency varies with load current, then the switching loss will also vary directly with load. This suggests that the standby-mode efficiency and battery current draw could be improved using a variable frequency approach.

At light load and low switching frequency, the converter circuits of Fig. 3 operate in the

discontinuous conduction mode (DCM), with the inductor current waveform diagrammed in Fig. 8. Each switching period of length $T_{sw}$ contains three subintervals. During the first, the MOSFET conducts, and energy is transferred from the battery to the inductor. During the second subinterval, the diode conducts, and the inductor stored energy is transferred to the load. At the end of the second subinterval, the diode becomes reverse-biased when the inductor current reaches zero. Both transistor and diode are off during the third subinterval, and the inductor current is zero for the remainder of the switching period. During the third subinterval, no conduction losses occur, and the only losses are due to leakage currents.

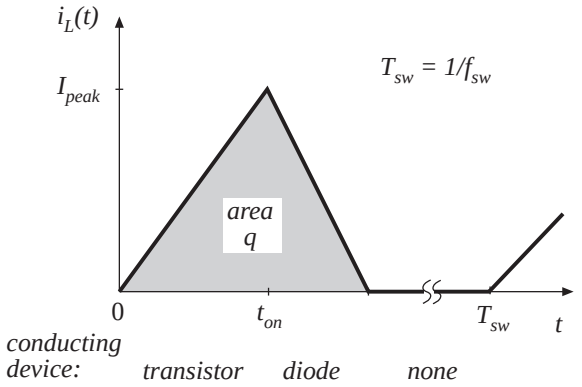


*Fig. 8. Inductor current waveform $i_L(t)$ in the discontinuous conduction mode.*

For a given transistor conduction time $t_{on}$, a fixed amount of energy per switching period is transferred to the load, given by

$$W_{load} = qV \tag{2}$$

where, for the buck converter, $q$ is the integral of the inductor current waveform and $V$ is the dc load voltage. The output power is then given by

$$P_{load} = W_{load} f_{sw} \tag{3}$$

In the process of transferring this energy to the load (during the first and second subintervals), some amount of energy $W_{loss}$ is lost as conduction and switching losses. To the extent that the fixed losses arising in the controller chip and due to leakage currents can be neglected, then the efficiency is given by

$$\eta = \frac{W_{load}}{W_{load} + W_{loss}} \tag{4}$$

Note that, if the quantities $W_{load}$ and $W_{loss}$ can be made independent of the load current, then the efficiency also becomes essentially independent of load current. There are several methods for accomplishing this, including constant on-time variable-frequency control, and constant peak current programming with variable frequency control.

In the constant on-time variable-frequency control scheme, the transistor on-time $t_{on}$ is fixed by the control circuit. As a result, the energy transferred to the load during one switching period, $W_{load}$, as well as the loss $W_{loss}$ incurred, are also fixed. The efficiency given by Eq. (4) is therefore independent of load current, and high efficiency occurs at light load. The output voltage is regulated by variation of the switching frequency $f_{sw}$.

Current programming is a popular means of controlling conventional dc-dc converters, and can also be used to control variable-frequency DCM converters [6] for battery-powered applications. Operation is similar to the constant-on time control scheme. However, rather than operating the transistor with a constant on-time $t_{on}$, the controller monitors the transistor current, and switches the transistor off when the transistor current reaches a predetermined level $I_{pk}$. The value of $I_{pk}$ is constant, and the output voltage is regulated by variation of the switching frequency. For given values of the inductance $L$ and the battery and load voltages, there is a direct relation between $t_{on}$ and $I_{pk}$.

How should $t_{on}$ or $I_{pk}$ be chosen? If these quantities are increased to large values, then high peak currents will occur, leading to large conduction losses. The converter will transfer a large amount of energy each switching period, and the converter will operate with low switching frequency. Alternatively, if $t_{on}$ or $I_{pk}$ are decreased to small values, then low peak currents will occur, with low conduction losses. However, a small amount of energy will be transferred each switching period, necessitating a high switching frequency with high switching losses. Hence, there is an optimum value of $t_{on}$ or $I_{pk}$ which leads to maximum efficiency.

Equation (4) was used to predict the efficiency of a dc-dc buck converter controlled by variable-frequency current programming. The same power stage elements assumed in section 2 to generate Figs. 6 and 7 were used. Efficiency is plotted as a function of peak transistor current in Fig. 9, with controller standby current and power stage leakage currents ignored. Depending of the choice of operating point, the converter may enter the continuous conduction mode at low values of $I_{pk}$; discontinuous conduction mode is assumed in generation of the figure. The efficiency is a mild function of the battery current,

however, the optimum efficiency occurs at approximately the same choice of $I_{pk}$ for a typical range of battery voltages. The optimum efficiency for this example occurs with a peak current of approximately one ampere. Experimental results presented in [1] confirm this behavior.

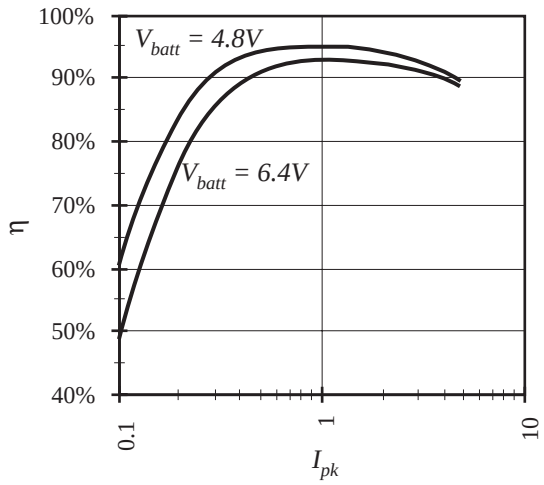


*Fig. 9. Efficiency vs. peak transistor current, for constant-current-programmed DCM buck converter example with variable-frequency control*

It is possible to further extend the useful range of load currents by allowing the converter to operate in the continuous conduction mode at high current. The switching frequency is increased, such that the third subinterval is eliminated. A sketch of switching frequency vs. load current is given in Fig. 10. Full load efficiencies greater than the value predicted by Eq. (4) are possible using this scheme.

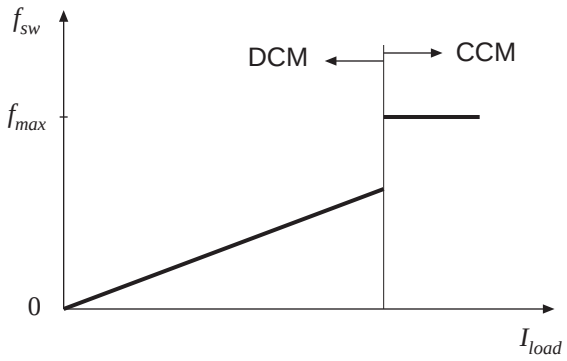


*Fig. 10. The operating range can be further extended by use of the continuous conduction mode near full load, and variable frequency discontinuous conduction mode at light load.*

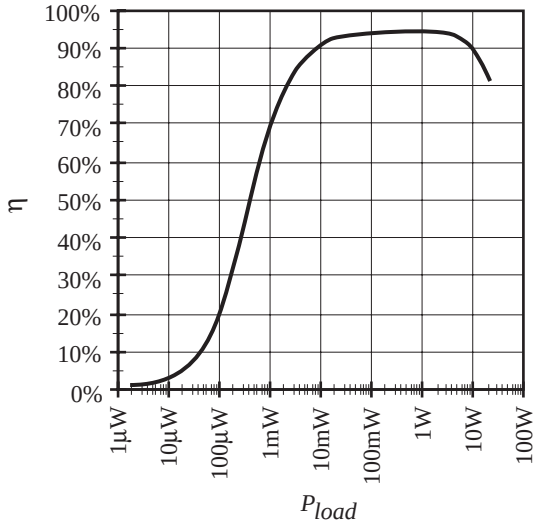


*Fig. 11. Predicted converter efficiency vs. output power, variable frequency converter.*

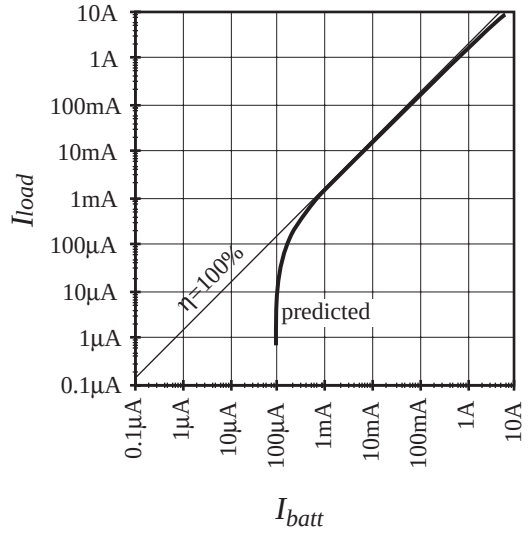


*Fig. 12. Predicted converter input current vs. output current, variable frequency converter.*

Efficiency and battery current are plotted vs. load power in Figures 11 and 12, for a well-designed variable-frequency switching converter. The same buck converter power stage elements used to generate Figs. 6 and 7 are assumed, and the converter supplies the same regulated 3.3V to a 0-25W load, from a four-cell battery pack having a minimum voltage of 4.8V. All sources of loss are modeled, including conduction and switching loss, leakage currents and controller standby current. For output powers greater than 2W, the converter operates in the continuous conduction mode with a fixed frequency of 100kHz. For output powers less than 2W, the converter

operates in the discontinuous conduction mode with variable-frequency current-programmed control. The peak current is then held constant at 1A.

By comparison of Figs. 6 and 11, it can be seen that the range of high efficiency ($\eta$>80%) is increased by approximately two orders of magnitude in load power. Efficiency greater than 80% is obtained for all load powers in the range 2.5mW – 25W. The no-load battery current is also decreased by nearly two orders of magnitude, from approximately 5mA in the conventional converter, to less than 100μA with the variable-frequency converter.

## 4. Characteristics of variable-frequency converters

The steady-state and small-signal ac behaviors of variable-frequency DCM converters are briefly summarized here, for both constant on-time and peak-current control.

For variable-frequency constant-on-time control, the converter voltage conversion ratio $M$ is given in Table 2 for the basic buck, boost, and buck-boost converters. The voltage conversion ratio $M$ is defined as

$$M = V / V_{batt} \tag{4}$$

The discontinuous conduction mode (DCM) occurs when the load current $I_{load}$ is less than the critical value $I_{crit}$, where

$$I_{crit} = (V_{batt} / R_e)\ (1-D)/D \tag{5}$$

for all three converters. The converters operate in continuous conduction mode (CCM) otherwise. $R$ is the load resistance, defined as $V/I_{load}$.

**Table 2. Summary of steady-state characteristics, variable-frequency constant on-time control**

| Converter | $M$ (CCM) | $M$ (DCM) |
|---|---|---|
| **Buck** | $D$ | $\frac{2}{1+\sqrt{1+4R_e/R}}$ |
| **Boost** | $\frac{1}{1-D}$ | $\frac{1+\sqrt{1+4R_e/R}}{2}$ |
| **Buck-Boost** | $-\frac{D}{1-D}$ | $-\sqrt{\frac{R}{R_e}}$ |

Duty cycle $D = t_{on} / T_{sw}$

Effective resistance $R_e = T_{sw}\, 2L / t_{on}^{\,2}$

The converter characteristics in steady-state for current programmed, variable frequency control are summarized in Table 3. Current programming tends to cause the converter output characteristic to approach that of a current source. The dc output current $I_{load}$ is listed in Table 3, as a function of the battery and load voltages, as well as the programmed peak current current $I_{pk}$ and the effective power $P$ defined as

$$P = \tfrac{1}{2} L I_{pk}^2 f_{sw} \tag{6}$$

It is assumed that the current mode controller does not contain an artificial ramp. The voltage conversion ratio $M$ and the critical current $I_{crit}$ are also listed; the boundary between continuous and discontinuous conduction modes is again given by $I_{load} = I_{crit}$.

**Table 3. Summary of steady-state characteristics, variable-frequency current mode control**

| Converter | $I_{out}$ (CCM) | $I_{out}$ (DCM) | $M$ (DCM) | $I_{crit}$ |
|---|---|---|---|---|
| **Buck** | $I_{pk} - \frac{V_{out}\,(1-V_{out}/V_{batt})\, I_{pk}^2}{4P}$ | $\frac{P}{V_{out}\,(1-V_{out}/V_{batt})}$ | $\frac{P_{out}-P}{P_{out}}$ | $\frac{1}{2} I_{pk}$ |
| **Boost** | $\frac{I_{pk}}{M}\left(1 - \frac{V_{out}\,(V_{out}/V_{batt}-1)\, I_{pk}}{4P}\right)$ | $\frac{P}{V_{batt}-V_{out}}$ | $\frac{P_{out}}{P_{out}-P}$ | $\frac{1}{2}\frac{I_{pk}}{M}$ |
| **Buck-boost** | $\frac{I_{pk}}{1-M}\left(1 + \frac{V_{batt}\, I_{pk}}{4P}\frac{M}{1-M}\right)$ | $\frac{P}{V_{out}}$ | Depends on load characteristic: $P_{out} = P$ | $\frac{1}{2}\frac{I_{pk}}{1-M}$ |

Voltage conversion ratio $M = V / V_{batt}$

Load power $P_{load} = V\, I_{load}$

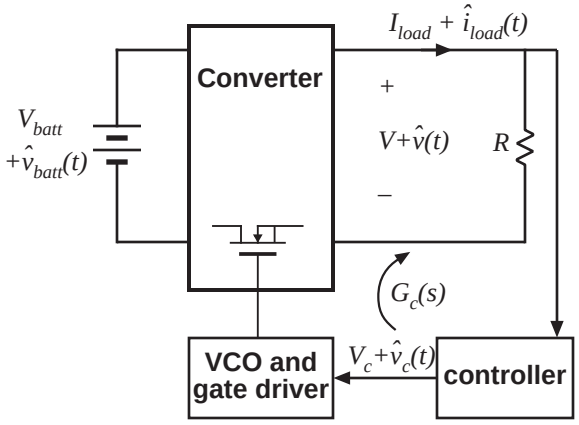


*Fig. 13. Output voltage regulation system block diagram.*

Design of the output-voltage-regulating feedback loop requires knowledge of the small-signal control-to-output transfer function, i.e., the transfer function $G_c(s)$ illustrated in the block diagram of Fig. 13. The output voltage is expressed as the desired steady-state quantity $V$ plus a perturbation $\hat{v}(t)$. The other signals are represented in a similar manner. The controller contains a voltage-controlled oscillator or equivalent device, whose small-signal gain is

$$K_{vco} = \frac{\hat{f}_{sw}}{\hat{v}_c} \tag{7}$$

where $\hat{f}_{sw}$ is the perturbation in the switching frequency caused by a control signal perturbation $\hat{v}_c$. By perturbation and linearization of the nonlinear averaged converter models, the two-port equivalent circuit model of Fig. 14 can be derived. General expressions for the two-port parameters are summarized in Tables 4 and 5, for DCM variable-frequency constant-on-time control and for DCM variable-frequency current-programmed control, respectively.

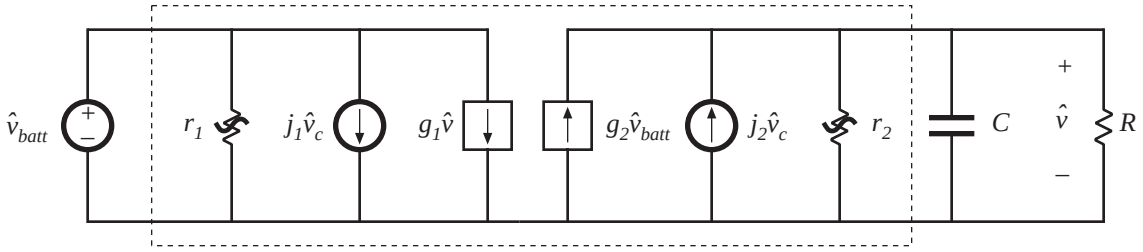


*Fig. 14. Equivalent circuit model which predicts the small-signal transfer functions of variable-frequency DCM converters.*

**Table 4. Small-signal model parameters, constant-on-time variable-frequency DCM**

| Converter | $g_1$ | $j_1$ | $r_1$ | $g_2$ | $j_2$ | $r_2$ |
|---|---|---|---|---|---|---|
| **Buck** | $\frac{-1}{R_e}$ | $\frac{V_{batt}\,K_{vco}}{R_e\,f_{sw}}(1\text{-}M)$ | $R_e$ | $\frac{(2\text{-}M)}{M\,R_e}$ | $\frac{V_{batt}\,K_{vco}}{R_e\,f_{sw}}\frac{(1\text{-}M)}{M}$ | $M^2R_e$ |
| **Boost** | $\frac{-1}{(M\text{-}1)^2\,R_e}$ | $\frac{V_{batt}\,K_{vco}}{R_e\,f_{sw}}\frac{M}{M\text{-}1}$ | $\frac{(M\text{-}1)^2}{M}R_e$ | $\frac{(2M\text{-}1)}{(M\text{-}1)^2\,R_e}$ | $\frac{V_{batt}\,K_{vco}}{R_e\,f_{sw}}\frac{1}{M\text{-}1}$ | $(M\text{-}1)^2R_e$ |
| **Buck-boost** | 0 | $\frac{V_{batt}\,K_{vco}}{R_e\,f_{sw}}$ | $R_e$ | $\frac{2M}{R_e}$ | $\frac{V_{batt}\,K_{vco}}{R_e\,f_{sw}}\frac{1}{M}$ | $M^2R_e$ |

**Table 5. Small-signal model parameters, variable frequency current programmed DCM**

| Converter | $g_1$ | $j_1$ | $r_1$ | $g_2$ | $j_2$ | $r_2$ |
|---|---|---|---|---|---|---|
| **Buck** | $\frac{\frac{1}{2}LI_{pk}^2 f_{sw}}{(V_{batt}-V)^2}$ | $\frac{\frac{1}{2}LI_{pk}^2\,K_{vco}}{V_{batt}-V}$ | $-\frac{(V_{batt}-V)^2}{\frac{1}{2}LI_{pk}^2 f_{sw}}$ | $-\frac{\frac{1}{2}LI_{pk}^2 f_{sw}}{(V_{batt}-V)^2}$ | $\frac{\frac{1}{2}LI_{pk}^2 V_{batt}\,K_{vco}}{V(V_{batt}-V)}$ | $\frac{V^2(V_{batt}-V)^2}{\frac{1}{2}LI_{pk}^2 f_{sw}V_{batt}\,(V_{batt}-2V)}$ |
| **Boost** | $-\frac{\frac{1}{2}LI_{pk}^2 f_{sw}}{(V_{batt}-V)^2}$ | $\frac{\frac{1}{2}LI_{pk}^2 V\,K_{vco}}{V_{batt}(V-V_{batt})}$ | $\frac{V_{batt}^2(V_{batt}-V)^2}{\frac{1}{2}LI_{pk}^2 f_{sw}V(2V_{batt}-V)}$ | $\frac{\frac{1}{2}LI_{pk}^2 f_{sw}}{(V_{batt}-V)^2}$ | $\frac{\frac{1}{2}LI_{pk}^2\,K_{vco}}{V-V_{batt}}$ | $\frac{(V_{batt}-V)^2}{\frac{1}{2}LI_{pk}^2 f_{sw}}$ |
| **Buck-boost** | 0 | $\frac{\frac{1}{2}LI_{pk}^2\,K_{vco}}{V_{batt}}$ | $\frac{V_{batt}^2}{\frac{1}{2}LI_{pk}^2 f_{sw}}$ | 0 | $\frac{\frac{1}{2}LI_{pk}^2\,K_{vco}}{-V}$ | $\frac{V^2}{\frac{1}{2}LI_{pk}^2 f_{sw}}$ |

By solving the equivalent circuit model of Fig. 14, one can derive the small-signal control-to-output transfer functions $G_c(s)$ of the various converters with the two control methods. In each case, the transfer function is quite simple, containing a single pole and a dc gain, of the form

$$G_c(s) = \frac{G_0}{\left(1 + \frac{s}{\omega_p}\right)} \qquad (8)$$

Expressions for $G_0$ and $\omega_p$ are collected in Tables 6 and 7. The quantity $K_{vco}$ is the controller gain, in Hz/volt.

The current-programmed buck converter operating in discontinuous conduction mode exhibits instability for voltage conversion ratios greater than 2/3. This instability was observed experimentally in [1]. Nonetheless, simple output voltage feedback can stabilize the system, resulting in good output voltage regulation. No instabilities occur in the other converters operating in discontinuous conduction mode.

**Table 6. Small-signal transfer function parameters, DCM constant on-time variable frequency control**

| Converter | Dc gain $G_0$ | Pole freq. $\omega_p$ |
|---|---|---|
| **Buck** | $\frac{V K_{vco}}{f_{sw}} \frac{(1-M)}{(2-M)}$ | $\frac{(2-M)}{RC\,(1-M)}$ |
| **Boost** | $\frac{V K_{vco}}{f_{sw}} \frac{(M-1)}{(2M-1)}$ | $\frac{(2M-1)}{RC\,(M-1)}$ |
| **Buck-boost** | $\frac{V K_{vco}}{2 f_{sw}}$ | $\frac{2}{RC}$ |

**Table 7. Small-signal transfer function parameters, DCM peak-current-programmed variable frequency control**

| Converter | Dc gain $G_0$ | Pole freq. $\omega_p$ |
|---|---|---|
| **Buck** | $\frac{V K_{vco}}{f_{sw}} \frac{(1-M)}{(2-3M)}$ | $\frac{(2-3M)}{RC\,(1-M)}$ |
| **Boost** | $\frac{V K_{vco}}{f_{sw}} \frac{(M-1)}{(2M-1)}$ | $\frac{(2M-1)}{RC\,(M-1)}$ |
| **Buck-boost** | $\frac{2V K_{vco}}{f_{sw}}$ | $\frac{2}{RC}$ |

## 5. Conclusions and future directions

Energy management allows increased capabilities in mobile battery-powered equipment, through the use of higher-powered components which are placed in a low-current standby mode when not needed. To realize the benefits of energy management, dc-dc converters must be capable of maintaining regulation of their output voltages at no load, while maintaining high efficiency. It is now feasible to build such converters, to supply a variety of load voltages from a single battery.

Variable frequency operation is shown to give an improvement in efficient operating range of approximately two orders of magnitude compared with the conventional constant-frequency approach. Proportionality of the battery and load currents can be maintained over approximately five orders of magnitude, with minimum battery currents of less than 100μA and maximum load currents approaching 10A.

Two variable-frequency control schemes are discussed here: constant on-time and current-programming. Steady-state behavior and small-signal ac transfer functions are given, as well as an ac two-port converter model.

At room temperature, the minimum battery current is essentially equal to the controller chip standby current. Additional work is needed to further reduce this current, and to implement improved control algorithms which allow optimized CCM and DCM operation. Efforts continue to integrate both controller and power semiconductor devices on the same chip, reducing size and cost.

Additional work in converter modeling and optimization could allow further improvements in size, efficiency, and usable power range. Other control schemes are also possible. Improvements in converter efficiency and noise generation may be possible using a resonant or other converter approach.

### REFERENCES


[1] B. Arbetter, R. Erickson, and D. Maksimovic, "DC-DC Converter Design for Battery-Operated Systems," *IEEE Power Electronics Specialists Conference*, 1995 Record, June 1995.

[2] M. Schlecht and L. Casey, "Comparison of the Square-Wave and Quasi-Resonant Topologies," *IEEE Applied Power Electronics Conference*, 1987 Record, pp. 124-134, March 1987.

[3] B. Huffman and R. Flatness, "Power Conversion from Milliamps to Amps at Ultra-High

Efficiency," Linear Technology Application Note 54, March 1993.

[4] "Battery Management and Dc-Dc Converter Circuit Collection —A Power Supply Application Guide for Portable Equipment," MAXIM Integrated Products, 1994.

[5] S. Cuk, "Modeling, Analysis, and Design of Switching Converters," Ph.D. Thesis, California Institute of Technology, Nov. 1976.

[6] R. Redl and N. Sokal, "Current-Mode Control, Five Different Types, Used with the Three Basic Classes of Power Converters: Small-Signal Ac and Large-Signal Dc Characterization, Stability Requirements, and Implementation of Practical Circuits," *IEEE Power Electronics Specialists Conference*, 1985 Record, pp. 771-785, June 1985.

[7] A. Dauhjare and R. D. Middlebrook, "A Simple PWM-FM Control for an Independently Regulated Dual Output Converter," Proceedings of POWERCON 10, March 1983.